The Meteoritical Society

Meteoritics & Planetary Science 47, Nr 10, 1681–1691 (2012)
doi: 10.1111/maps.12004

The effects of meteorite impacts on the availability of bioessential elements for endolithic organisms

Alexandra PONTEFRACT[1*], Gordon R. OSINSKI[1], Paula LINDGREN[2], John PARNELL[3], Charles S. COCKELL[4], and Gordon SOUTHAM[5]

[1]Department of Earth Sciences, University of Western Ontario, London, Canada
[2]School of Geographical and Earth Sciences, University of Glasgow, Glasgow, UK
[3]Department of Geology, University of Aberdeen, Aberdeen, UK
[4]School of Physics and Astronomy, University of Edinburgh, Edinburgh, UK
[5]School of Earth Sciences, University of Queensland, St. Lucia-Brisbane, Australia
[*]Corresponding author. E-mail: apontefr@uwo.ca

(Received 13 April 2012; revision accepted 14 September 2012)

Abstract–Meteorite impacts, one of the most ubiquitous processes in the solar system, have the ability to destroy as well as create habitats for life. The impact process can increase the translucency and porosity of the target substrate, as well as mobilize biologically relevant elements within the substrate. For endolithic organisms, this process has important implications, especially in extreme environments where they are forced to seek refuge in the interior of rocks. Here, we show that unshocked target rocks and rocks that have experienced pressures up to about 80 GPa from the Haughton impact structure, Devon Island, Canada, possess a small, but discernible change in bulk chemistry within the major oxide analysis. However, changes in the distribution of elements did occur with increasing shock level for both the sedimentary and crystalline target. Both the crystalline and sedimentary target rocks contain significant amounts of glasses at higher shock levels (up to about 95% by volume), which would improve the availability of these elements to potential microbial endoliths as glasses are more easily dissolved by organic acids. The implication that impact events do not impoverish their capacity to serve as a "substrate" through volatilization is important with respect to analogous impact structures on Mars. After the deleterious effects of the direct meteorite impact, any microorganisms on Mars would have benefited from the input of heat, the mobilization of a possible frozen groundwater system, as well as increased translucency, porosity, and trace nutrient availability of the target substrate.

INTRODUCTION

Meteorite impact events are capable of generating extreme temperatures and pressures, causing the target substrate to undergo deformation, vaporization, melting, and shock metamorphism. Although initially destructive in nature, these processes can favorably change the habitability of the target substrate for rock-dwelling (endolithic) organisms, which are able to (re)colonize fractures and pore spaces created by the impact (Cockell et al. 2005). Of further interest are the generation of postimpact hydrothermal systems and the role they play in hosting microbial life. Previous work has revealed the creation of hydrothermal systems immediately following an impact into a H_2O-bearing substrate (e.g., Naumov 1996; Osinski et al. 2012). These systems, depending on the size of the impactor, are capable of being active for up to several million years in large (100 km-scale) impact craters (e.g., Ames et al. 1998). When considering the current view that the origins of life are rooted in high temperature systems (Martin et al. 2008), as well as the continuity of impact events throughout the lifetime of a planetary body, it is plausible that such impact-generated systems could have played host to the origins of life on Earth, as well as on other bodies in the solar system (e.g., Osinski et al. 2001, 2005; Cockell and Lee 2002; Cockell 2004; Versh et al. 2006; Parnell et al. 2010).

The formation of communities in the interior of rocks (hereafter referred to as endolithic) has long been recognized as an advantageous response to harsh environmental conditions, especially in relation to cold, arid environments such as polar deserts (Friedmann and Ocampo 1976; Friedmann 1980; Vestal 1988; Wierzchos and Ascaso 2001). These habitats can be created through a variety of processes: physical, chemical, and biological. Organisms residing in, upon, or beneath these lithic habitats generally enjoy increased UV protection, shelter from wind ablation and temperature shifts, as well as benefitting from the build-up of wind-blown debris, which often serves as a source of nutrients (Friedmann 1980). Finally, endolithic communities (both phototrophic and heterotrophic) are capable of acquiring their nutrients directly from the substrate itself (Konhauser 2007). Redox reactions occurring at the rock–water interface can provide fuel for microbial metabolism. Microbes themselves can also alter the chemistry of the environment through the production of organic acids, which aid in weathering the substrate (Konhauser 1998).

Given the benefits of an endolithic way of life in response to extreme environmental conditions, it has been posited that endolithic organisms could exist (or have existed) within impact craters on planets such as Mars (Cockell and Lee 2002) and/or within the deep Martian sub-surface (Boston et al. 1992). Studies by Cockell et al. (2002, 2005) and Cockell and Osinski (2007) have shown that growth of endoliths within impact-metamorphosed substrates correlates with shock level in both sedimentary and crystalline targets; however, the specifics of this relationship are still unclear. Increased porosity and translucence of the substrate may be major contributors to this relationship, but what is still unknown is the scaling of available nutrients with an increase in shock level. In particular, upon exposure to temperatures up to, and exceeding 2000 °C, the target may experience redistribution or loss of elements essential for microbial metabolism. Importantly, there are six major elements that are necessary for life: C, H, N, O, P, and S; as well as several that play key roles in DNA synthesis (mechanistic or enzyme function), cell membrane stability, pH balance, ion transport, and enzymatic digestion such as Cl, K, Na, Mg, Mn, Fe, Cu, Co, Ni, Zn, and Se (Wackett et al. 2004). Many of these are present as hydrated oxides within rocks and, as such, are subject to volatilization during an impact event.

The purpose of this study is to determine whether element redistribution or element loss occurs within the target as a result of a meteorite impact, to elucidate the capability of a shocked target to provide sufficient major and trace elements to support microbial colonization (with the exception of N, which was not studied here since it can be "easily" fixed by bacteria in endolithic habitats; Boison et al. 2004) to support microbial colonization. Preliminary work by Fike et al. (2003) showed a potential loss in bioessential elements in a study of crystalline rocks; however, later work by Lindgren et al. (2007) and Osinski et al. (2010), presented only in abstract form, suggested that there was no significant loss of bioessential elements in carbonaceous samples. We present new data on crystalline rocks and a synthesis of previous published and unpublished geochemical work completed on extensive data sets of both crystalline and sedimentary samples. To this end, the study of a relatively young and unaltered impact structure was necessary, and was satisfied by the Haughton impact structure in the Canadian High Arctic.

Field Site

The Haughton impact structure is located on the northwestern region of Devon Island, Nunavut, in the Canadian High Arctic archipelago at 75°08′N, 87°51′W (Osinski et al. 2005a). This 39 Ma complex impact structure has been well documented, with studies going back to the 1970s (e.g., Frisch and Thorsteinsson 1978; Grieve and Robertson 1979). The target rocks are almost entirely sedimentary and represent lower Paleozoic rocks of the Arctic Platform. This approximately 1880 m sequence (preimpact thickness) is comprised of carbonates, with lesser amounts of evaporites, sandstone, and shale, overlaying gneisses of the Precambrian basement of the Canadian Shield (Fig. 1). Haughton has an apparent diameter of about 23 km, with a final crater rim estimate of 16 km in diameter (Osinski et al. 2005). The most identifiable feature of the impact structure is the pale-gray crater-fill (clast-rich impact melt rocks) deposits, which form a discontinuous layer throughout the center of the structure. Another salient feature of the structure is its hydrothermal deposits, seen in the form of several alteration products, such as selenite and marcasite, as well as the presence of hydrothermal vugs (Osinksi et al. 2001, 2005b). Finally, lacustrine deposits comprising the Haughton Formation are present in and around the center of the crater, which represent the transient presence of a lake during the Neogene several Myr after the crater formed. These sediments contain fossilized pollen grains, plants, and vertebrate skeletons, and represent a late stage in the biological succession of the crater (Cockell and Lee 2002).

METHODS

Sample Collection and Processing

Samples for this study were collected during field seasons from 1999 up until 2010 from many different

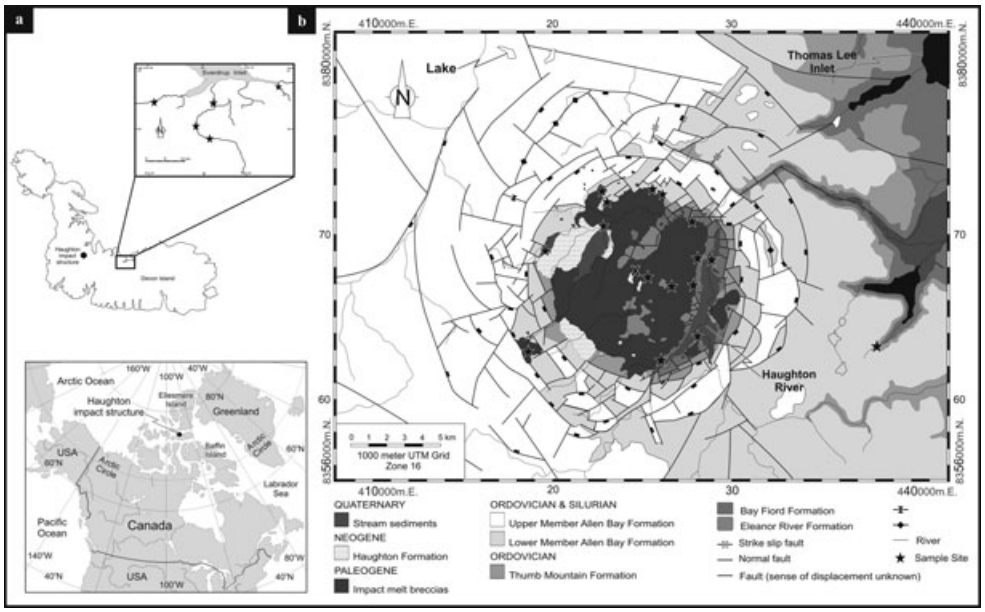

Fig. 1. a) Map showing location of the Haughton impact structure on Devon Island, as well as the location of Sverdrup Inlet (top). b) Target stratigraphy in and around the Haughton structure. Modified after Osinski et al. (2005a). Sample sites for all data sets are shown as black stars both within and outside of the crater (a, b). Note that in some cases, multiple sites are represented by one marker due to their proximity. For detailed coordinates of each site, see Table S2.

locations within and exterior to the crater, and consist of three separate suites (Fig. 1).

Suite 1: Total Organic Carbon (TOC) Analysis

The samples of target bedrock that were analyzed for TOC came from a wide range of preimpact depths in the sedimentary target succession and include material from different formations: Allen Bay Fm, Thumb Mountain Fm, Bay Fiord Fm, Eleanor River Fm, and Blanley Bay Fm (Fig. 1). This corresponds to 10 samples of target carbonate, two samples of target sulfate, four samples of target sandstone, and four samples of target shale. From the impact products, five samples of whole clast-rich melt rock from four different localities, and six lithic carbonate clasts in the clast-rich melt rock, from six different localities, were analyzed. In addition to measuring the total organic carbon in the whole clast-rich melt rock, lithic carbonate clasts, with sizes of a few cm in diameter were analyzed, to investigate the amount of organic carbon preserved after the carbonate clasts had been affected by a high temperature impact melt.

Suite 2: Sedimentary Target Analysis

Sedimentary samples corresponding to (1) unshocked, (2) low shock, (3) clast-rich melt rock (CMR), (4) CMR clasts, and (5) postimpact sediments, were collected from several different units both within and outside of the crater. These samples were powdered using a pulverizer, and analyzed using X-ray fluorescence spectroscopy (XRF) (see below).

Suite 3: Crystalline Target Analysis

Crystalline (gneiss) samples representing the unshocked basement were collected from in and around Sverdrup Inlet (see Fig. 1a). It is important to note here that we have assumed that the composition of the basement under the crater and the basement at Sverdrup Inlet is the same, but it is possible that significant heterogeneity is present. Shocked samples were collected within the crater from a wide number of locations on several of the breccia hills located both near the crater rim and toward the central uplift. These samples were thin-sectioned. Shocked samples were powdered using an alumina mortar and pestle (CoorsTek, Colorado, USA #60370). Samples from the unshocked crystalline basement were crushed using a Bico Chipmunk Crusher, and powdered using a T.M. Vibratory Ring Pulverizer. These samples were then analyzed using inductively coupled plasma (ICP) emission spectroscopy (see below).

Shock Classification

Shock classification of crystalline rocks was done through the use of petrographic analysis (Fig. 2). This process was necessary so as to determine the extent of alteration experienced by each sample, allowing for a correlation between the extent of heat and pressure that the substrate was exposed to and any corresponding changes in bulk chemistry. In this paper, we have used the classification system created by Singleton et al. (2011) for rocks at the Haughton structure, which expands on

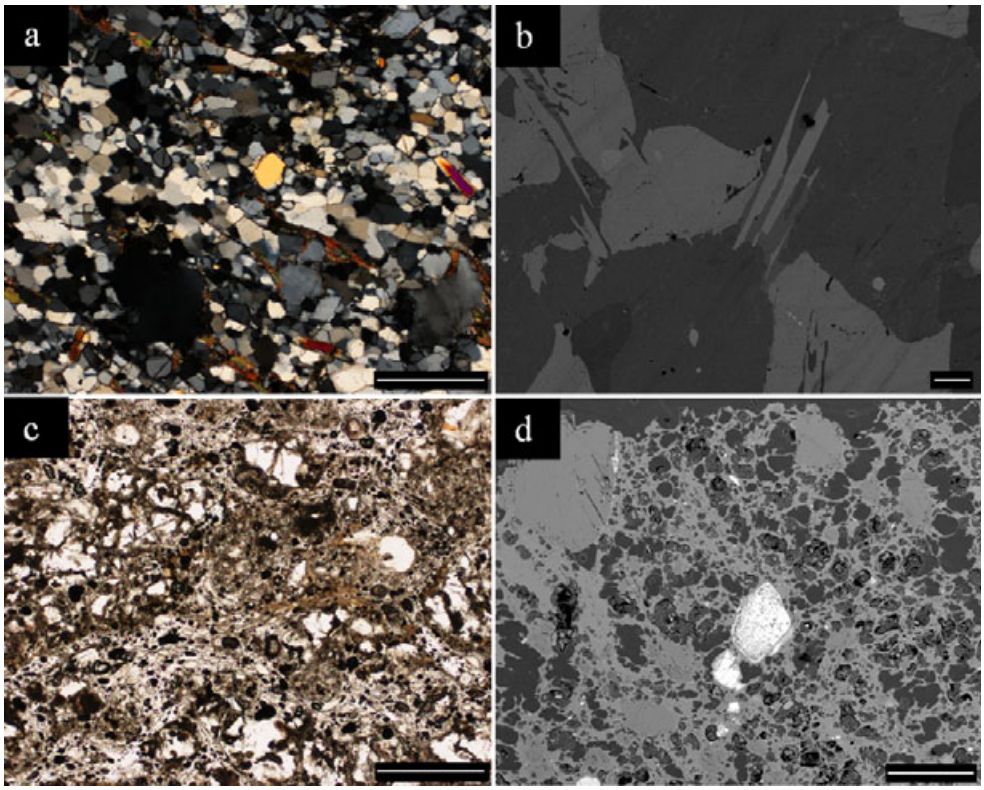

Fig. 2. Photomicrographs and backscattered electron images of crystalline gneiss. Figures 2a (under cross-polarization) and 2b (SEM-BSE) show unshocked crystalline basement from Sverdrup Inlet. The sample is largely comprised of quartz, plus silliminite and biotite. Figures 2c (plane polarized) and 2d (SEM-BSE) are samples of gneiss of shock level 6 shocked at upwards of 60 GPa. Note the extensive frothy texture and presence of glass phases. Scale bars for light micrographs (a, c) are 500 μm, scale bars for SEM-BSE micrographs (b, d) are 100 μm.

work by Stöffler (1966, 1971), Chao (1968), Metzler et al. (1988), Bunch et al. (1997), and French (1998) (see Table S1). This new classification system refines the earlier shock level demarcations, dividing them into a much finer-scale classification and allowing for a more in-depth investigation of correlative analyses. The classification system used in this article for the crystalline strata cannot currently be applied to the sedimentary strata due to significant differences in the response of the lithology to shock. For a comparison of shock between carbonate and crystalline targets, see Osinski (2007). Shock classification schemes for carbonate rocks do not currently exist. It should be noted that in this article broad terms referring to shock are sometimes used, i.e., ''unshocked'' refers to shock level 0 samples, ''low shock'' to shock levels 1–4, and ''high shock'' to shock levels 5–7.

TOC

Samples were analyzed either through acquiring a powder by drilling out the components of interest, or crushing them to a fine powder using a TEMA mill after trimming the edges of the samples with a diamond saw blade to remove surface weathering and contamination. Before analysis, the carbonate-bearing samples were treated with warm 25% hydrochloric acid (HCl) for removal of inorganic carbon (Gross 1971). The acid residues were analyzed with a carbon-sulfur analyzer (LECO CS225) at the University of Aberdeen for their total organic carbon content. Preimpact target rocks from outside the crater were sampled and compared with the clast-rich melt rock. The composition of the CMR was assumed to be approximately 74% carbonates, 10% evaporates, 8% sandstone, and 8% shale, based on the preimpact stratigraphy between 500 and 2000 m.

XRF

Analyses were carried out on a PHILIPS PW2440 4 kW automated XRF spectrometer system by Geochemical Laboratories, McGill University, Montréal, Canada. This system uses a rhodium 60 kV end window X-ray tube, five X-ray detectors, four primary beam filters, eight analyzing crystals, two fixed channels for simultaneous measurement of Na and F, and a PW2540 168 sample *x–y* autochanger. The major elements were analyzed using 32 mm diameter fused beads prepared

from a 1:5 sample: lithium tetraborate mixture. Minor element analyses were performed on 40 mm diameter pressed pellets prepared from a mixture of 10 g sample powder with 2 g Hoechst Wax C Micropowder. Data sets were analyzed for statistical significance using a nonparametric Mann–Whitney *U*-test, which is similar to the *t*-test for determining whether two populations are statistically separate; however, it does not assume any specific distribution of the data, unlike the *t*-test which requires a normal distribution (Mann and Whitney 1947; McKnight and Najab 2010).

ICP

Analyses of major oxides and trace elements were done using a Perkin Elmer Elan ICP-MS by Acme Labs, Vancouver, Canada. Powdered samples were prepared in a lithium metaborate/tetraborate infusion, and then dissolved using ACS grade nitric acid. Loss on ignition (LOI) was determined by igniting a sample split, then measuring the weight loss. Total carbon and sulfur were determined using a Leco Carbon-Sulfur Analyzer; samples were ignited in an induction furnace and adsorption of carbon/sulfur was measured by an infrared spectrometric cell. Detection limits for all of the major oxides were at 0.01%, with Cr_2O_3 at 0.002%. The data set for trace element composition is limited to ICP data, as the XRF study did not include this analysis. Data sets were analyzed for statistical significance using a nonparametric Mann–Whitney *U*-test, for non-normally distributed populations.

SEM-BSE and EDX Analysis

Polished thin sections of gneiss from each of the shock levels were imaged to identify any trends in the redistribution of major element composition with increasing shock. Areas of interest (regions containing vesicles and/or melt) were first identified using a petrographic microscope. Samples were carbon coated using an Edwards Auto 306 and imaged on a Hitachi SU6600 Analytical FEG-SEM (scanning electron micrograph), using a 5 segment back-scatter (BSE) detector. Semi-quantitative chemical information was collected using an Oxford 80 mm^2 XMax electron dispersive X-ray (EDX) detector, and analyzed using Inca Microanalysis Suite, v. 4.11.

RESULTS

TOC in Haughton CMR

The total organic carbon in the various target lithologies and impact products at Haughton are presented in Table 1 (see also Table S3). Both the carbonate clast fraction of the melt rock and the whole rock samples of melt rock contain low levels of organic carbon; 0.10–0.17% TOC, with an average value of 0.14%. This is substantially lower than the contribution of organic carbon measured as an input from the preimpact target rocks, i.e., 0.66%; however, we found that the preimpact sandstone target has a total organic carbon content that varies between 0.03% and 0.06%, which is lower than the melt rock values. The two samples of sulfate analyzed here have values of 0.13% and 0.03% TOC, respectively, We also found that organic carbon input to the CMR from the target was highly dependent on the shale (see Table S3), which has a preimpact TOC of up to 11.43%, although samples of CMR only preserved 20% TOC on average (Table 1).

Table 1. Calculation of total organic carbon contents (TOC).

Target bedrock	% TOC	Lithology contribution to clast-rich melt rock (%)	% TOC input from the target bedrock
Carbonate (10)	0.12 (*0.07*)	74	0.09
Sulfate (2)	0.08 *n/a*	10	0.01
Sandstone (4)	0.05 (*0.01*)	8	0.004
Shale (4)	7.01 (*5.26*)	8	0.56
			Sum: 0.66

% TOC target input	% TOC melt rock (5)	% TOC preserved in CMR	% TOC target carbonate (10)	% TOC carbonate clasts (6)
0.66	0.14	~20	0.12	0.14

The numbers within the parentheses represent the number of different samples that were analyzed. Italicized numbers located adjacent to % TOC values represent the standard deviation of the sample. See Table S3 for full data set.

Sedimentary Samples

A total of 57 samples were analyzed through XRF analysis (Table S4). For all of the major oxides analyzed, none of these "bulk" samples showed any relationship with shock level, with P actually showing higher concentrations in postimpact sediments (about 0.07%) and impact melt breccia, than in the unshocked/low shock samples (about 0.03%) (Fig. 3). Many of the major oxides were close to, or at, the detection limits. In Figs. 3b and 3c, there is an excellent correlation of Fe_2O_3:Al_2O_3 and P_2O_5:Al_2O_3 (irrespective of shock level, with the exception of the postimpact sediments, some of which fall off the line), with R^2 values of 0.9707 and 0.9742, respectively, and $P < 0.01$ for both. Figure 3a shows no correlation, and is largely representative of the bulk of the data collected.

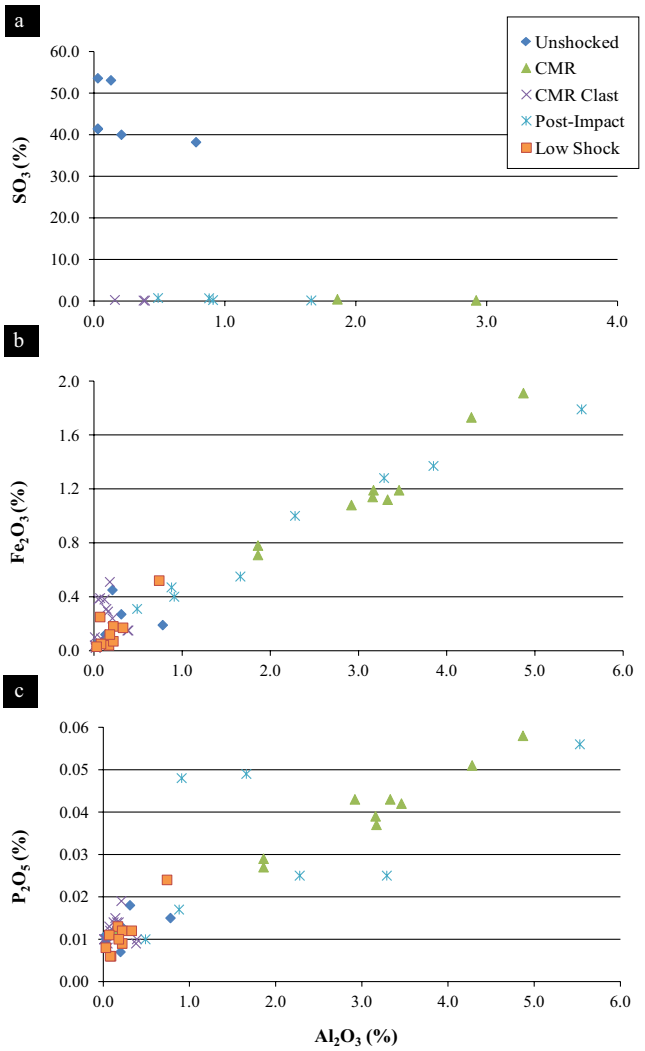

Fig. 3. Graphs showing XRF data of sedimentary lithologies for some biologically relevant elements, plotted against Al_2O_3. In Figs. 3b and 3c, a trend is visible with with R^2 values of 0.9707 and 0.9742 respectively.

Crystalline Samples

Fifty samples of both shocked and unshocked gneiss from in and around Haughton were analyzed through XRF and ICP, the data of which was plotted together, as the two methods were found to be in good agreement (Table S5a,b). From both the major oxide and trace element data collected, no fine-scale correlation between shock level and elemental composition was found. Indeed, samples from low-shock and high-shock levels frequently had the same composition (Fig. 4). Elemental composition was also plotted against broad-range shock levels (i.e., unshocked versus low shock), which revealed a reduction in elemental concentration with increasing shock pressure. The preimpact composition of the gneisses in and around the Haughton structure are quite variable, with at least 11 different types of gneiss identified (Metzler et al. 1988). This heterogeneity of target materials is represented in our own sample set of 10 unshocked basement rocks, where Si content varied from 50% to 80%, and Fe ranged from 1% up to 9%. In addition, data sets were also plotted as a set of means for each major oxide and trace element analyzed, standard deviations are available in Table S5a,b. For all of the major oxides, with the exception of SiO_2 and CaO, the mean concentration decreased with increasing shock level, revealing a polynomial distribution (Fig. 5). A polynomial trendline was fitted to the data, with the highest correlation being MgO, $R^2 = 0.8625$, see Fig. 4. The highest concentration levels were observed not in the unshocked samples, but in samples from shock level 3 (10–30 GPa range), which was found to be a statistically different population, $P < 0.05$ from all of the other samples (see Table S5c for probability calculations).

SEM-BSE and EDX

Although changes in bulk chemical composition were minor, it is evident that there was significant redistribution of these elements, especially at higher shock levels. BSE images from shock levels 5 and above (Fig. 6), show large amounts of feldspar mineral glasses. Generally, these glasses contain quartz clasts that still preserve their grain shapes, as well as partially melted plagioclase and K-feldspar clasts (Fig. 6a). In some cases, the glasses contain small, 1–10 μm-scale, iron and titanium-rich clasts (Fig. 6b). We were not able to determine the mineralogy of these clasts.

DISCUSSION

As the shockwave passed through the preimpact target of the Haughton structure, temperatures and pressures upwards of 2000 °C and about 80 GPa, respectively, were likely attained (Osinski et al. 2005b). One hypothesis is that the intense volatilization and melting that occurred as a result of this impact and the concomitant loss of material would have a similar effect on labile elements in the target substrates, i.e., a depletion of oxides, resulting in brecciated samples that were composed primarily of Si and O. This would of course have significant deleterious effects on the ability of microorganisms to inhabit such environments. We find, however, that this is not the case. In our analysis of over 100 samples of sedimentary and crystalline rocks, no systematic change between differing shocked samples in either the major oxide or trace element data sets were observed when plotted as ratios. For some of the major oxides within the crystalline samples, a significant difference was noted between unshocked and highly

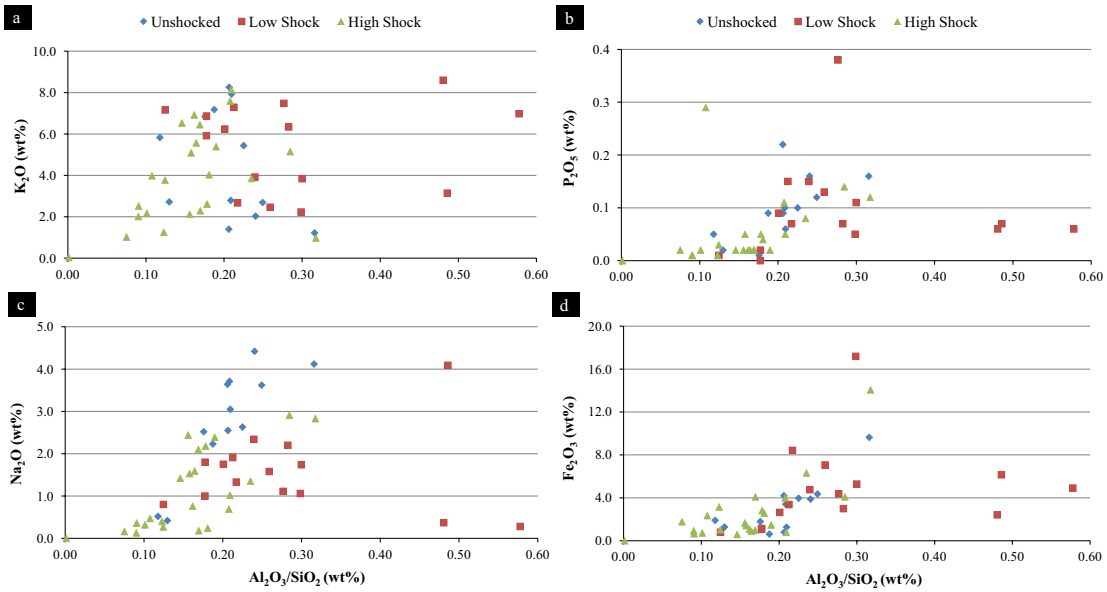

Fig. 4. Graphs showing combined XRF and ICP data for crystalline rocks of various elements plotted against the ratio of Al_2O_3/SiO_2. With the exception of Na_2O, the other graphs show no significant difference between unshocked and low shock populations. All four plots show a statistical difference ($P < 0.01$) between the low-shock and high-shock populations which reveal a reduction in concentration for the given element.

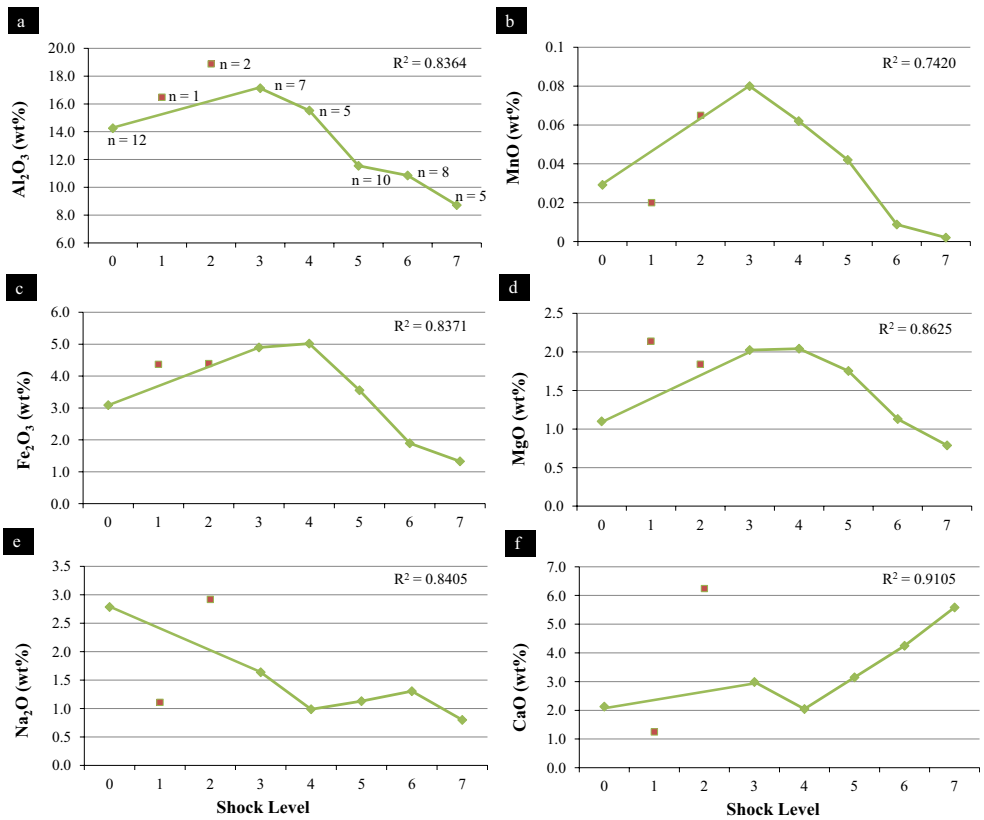

Fig. 5. Graphs showing the means of several different elements, compiled from XRF and ICP data (see Table S5a). Shock levels 1 and 2 (shown here as discrete separate points) have been omitted from this analysis, as they only comprise 1 and 2 samples, respectively, and as such, are subject to a significant amount of bias. For all of the graphs the unshocked samples were shown to be statistically different from shock level 3 samples. A significant difference was also observed between shock level 3 and 7 sample populations. See Table S5c for all *P*-value calculations.

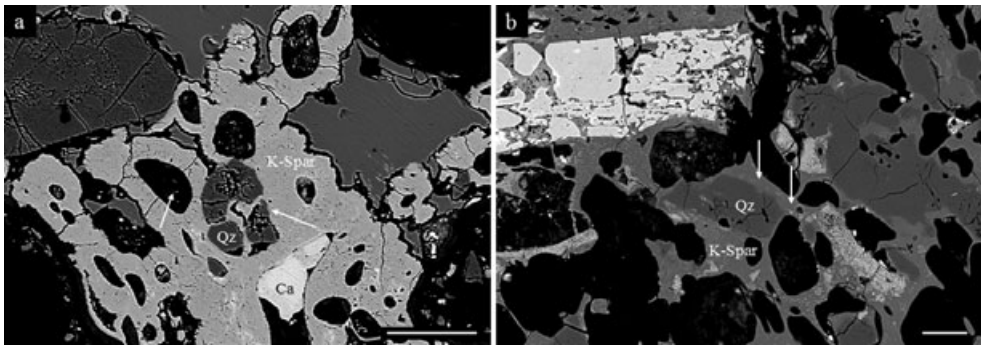

Fig. 6. SEM-BSE micrographs of shocked gneiss. Both images show quartz (Qz) clasts within a mineral glass derived from potassium feldspar (K-Spar). In (a), the left-most arrow highlights a vesicle, and the right-most, an area where the quartz crystal has been disaggregated into ''rafts'' within the glass. In (b), the arrows indicate where small amounts of iron have been mobilized within a feldspar mineral glass. Scale bars are 100 and 10 μm, respectively.

shocked samples, and in some cases between low-shock and high-shock samples (Figs. 4a and 4c). Alternatively, within the sedimentary samples, some of the values are actually found to be higher within shocked samples (Fig. 3a). In the case of phosphorus, the higher levels of the shocked samples may be the result of phosphate deposition from hydrothermal fluids or could be derived from input of the basement materials (e.g., from apatite-bearing granitic lithologies). Another potential source of phosphorus within the rocks analyzed could, intuitively, be due to the phosphorus within the colonizing organisms, all of which require phosphorus for cellular function (Oberson and Joner 2003). This would also explain why the hydrogeochemically isolated CMR clasts do not show an increase in phosphorus, as the CMR clasts would not be exposed to endolithic colonization. However, it does not answer where these organisms got their phosphorus. If it came from the host rock, then isolated CMR clasts should have also been enriched in phosphorus.

Mean values of the data for all samples (both sedimentary and crystalline) were calculated, but it was only when plotting the means of the major oxides for the crystalline samples that a decrease in concentration with shock level was observed (see Fig. 5). This was not seen in either the trace element data for the crystalline samples, or in any of the sedimentary material. The explanation for this is unclear. It is possible that the trace elements themselves are generally a part of more stable phases within the rock and thus are not so readily volatized. However, with the sedimentary data, this is likely not the case. One important difference between the sedimentary and crystalline data, however, is the classification system that is used. The lack of a fine-scale, i.e., micrometer-scale, categorization of shock level in sedimentary lithologies then, may be limiting our ability to detect changes occurring within the current broad categorization used.

Curiously, most of the oxides for the crystalline samples experience a peak in mean concentration at shock level 3 and then begin to decrease beyond this. As noted previously, we have assumed that the basement samples collected from Sverdrup Inlet (representing unshocked gneiss) have the same composition as those beneath the impact structure. Given that most of the unshocked samples (with the exception of Fig. 5f) plot below the shocked samples, it is likely that some heterogeneity is present. Shock level 0 samples were shown to be statistically different from the shock level 3 suite of rock, but frequently were considered to be quite similar to the shock level 7 grouping (see Table S5c). Given that shock level 3 was statistically different from shock level 7, we believe that this clearly shows that the unshocked basement outside the crater is not ideally representative of the preimpact basement beneath the crater. Unfortunately, there is no other way to access the preimpact basement and so we must use the values collected. In some of the graphs (e.g., Figs. 5a and 5d), the values for shock levels 1 and 2 (which were omitted from the trend line due to insufficient sample numbers) plot above the higher shock levels, supporting the idea that the lower shock levels (i.e., shock levels 1–3) possess increased nutrients relative to their more highly shocked counterparts (this does not, however, inhibit endolithic growth; Cockell et al. 2002). The lack of low-shock samples in this study is representative of the fact that there is a significant paucity of low-shock samples available from the Haughton structure in general. This deficiency has been noted in previous studies of the structure (e.g., Metzler et al. 1988), but to date the reasons are still unclear. It should also be noted that the decrease seen in the mean data could have alternative explanations. It is possible, for example, that the decrease is representative of the path of the shockwave, traveling through different lithologies as it radiates out from a central point.

When examining the major physical changes occurring in the crystalline samples, significant change is

found to occur at the transition from shock levels 4 and 5. At this point, one can see the formation of diaplectic glasses as well as selective melting of some minerals. It follows then that at this stage there could be mobilization of elements occurring within the samples, which would explain any decrease in oxide composition. Indeed, at shock level 6 we observed feldspathic- and silica-rich glasses that were intermingled, although still appearing to maintain distinct boundaries (Fig. 6b). Within these melts, we also observed small titanium and iron-rich clasts that were possibly mobilized as a result of the heat and pressure. Taking into account the problems inherent with collecting sufficient chemical data for the lower shock levels, it is plausible that concentrations might actually remain fairly consistent up until shock level 4, and then begin to experience a more significant decrease. Finally, it is noted that in Fig. 5f, there is actually an increase in the concentration of CaO with shock level. There could be several reasons for this. First, the CaO could be present as carbonate melt inclusions, which forms the groundmass to the impact melt rocks (Osinski et al. 2005a). Alternatively, these elevated CaO levels could be the result of postimpact alteration (either through hydrothermal or modern-day weathering), where increased pore space with increasing shock levels would allow for more significant amounts of secondary carbonate deposition.

The TOC data from the carbonate clasts of the CMR exhibit a similar pattern. The results from the TOC analysis and the mass balance calculation of carbon in the target before impact and carbon preserved in the carbonates show that the organic carbon levels actually increase. The carbon input to the CMR from the preimpact target, however, is highly dependent on the carbonate target rock, since 74% of the target succession is composed of carbonate. The results from the TOC analyses show that the carbon content of the carbonate target varies significantly between different samples (0.07–0.30% TOC), while the carbon content of the melt rock is more constant (0.10–0.17% TOC) which is not a significant change. This is likely a result of the fact that the melt rock is a mix of all target rocks, and therefore the %TOC is averaged out here. These values are consistent with previous studies that have shown that despite the high initial temperatures of the impact melt rocks (>1750 °C for Haughton [Osinski et al. 2005b]), organic carbon is preserved in the impact melt breccia, including in the lithic carbonate clasts (Parnell et al. 2005).

Biological Implications

The ability of organisms to derive nutrients from the lithosphere (nutrients that are largely unavailable to many living organisms) has been long documented (Barker et al. 1997; Ehrlich 1998; Welch et al. 1999; Bennett et al. 2001; de los Ríos et al. 2002; Konhauser 2007; Omelon 2008). Many microorganisms are capable of secreting a wide range of organic acids and chelators to liberate elements from mineral surfaces. Exopolysaccharide (EPS) can maintain acidity levels and act as binding cites for mineral formation (Barker et al. 1997; Douglas and Beveridge 1998). Some minerals, however, can prove difficult to dissolve due to the stability of their crystal structure. The observation that levels of microbial growth tend to increase with shock level (e.g., Cockell and Osinski 2007) correlates, in part, with the occurrence of glasses within the impact-shocked rocks. The answer for this may lie in the amorphous nature of glasses, which are more easily weathered due to the lack of a stable crystalline framework, promoting the growth of these microorganisms. For example, the mobilization of iron into the melt would intuitively make it more accessible to the microbial community (Fig. 6). In addition, during mobilization and potential volatilization of hydrous minerals, the corresponding elements, such as K, Na, and Mg that are left behind, might preferentially coat the insides of vesicles (Fike et al. 2003).

CONCLUDING REMARKS

This study has shown that, although initially very destructive, a meteorite impact event does not cause impoverishment of the target substrate with respect to elements essential for life (as we know it). Coupled with the formation of possible hydrothermal systems, an increase in available habitat for endolithic organisms and the generation of heating over a long (million-year) period of time, it is possible that impact craters could serve as habitats for life on other planets than our own. As these hydrothermal environments began to cool down and eventually disappeared entirely, putative microbial colonies could have migrated into these newly created endolithic habitats where they would be protected from UV radiation, temperature shifts, and dessication. If this hypothesis proves accurate, it is plausible that dormant or fossilized colonies of such organisms exist today, buried under overlying millennia of deposition.

Acknowledgments—This project was funded by the National Sciences and Engineering Research Council (NSERC), the Northern Scientific Training Program (NSTP), the Canadian Astrobiology Training Program (CATP), and the NSERC/MDA/CSA Industrial Research Chair in Planetary Geology held by GRO. Thank you to the Polar Continental Shelf Project for logistical and technical support. Thank you also to Ivan Barker, Radu-Dan Capitan, Haley Sapers, Livio

Tornabene, Louisa Preston, and Matthew Izawa for their helpful comments in completing this manuscript. Finally, thank you to C. Koeberl, C. McKay, and an anonymous reviewer for their valuable and constructive comments toward improving this manuscript.

Editorial Handling—Dr. Christian Koeberl

REFERENCES

Ames D. E., Watkinson D. H., and Parrish R. R. 1998. Dating of a regional hydrothermal system induced by the 1850 Ma Sudbury impact event. *Geology* 26:447–450.

Barker W., Welch S. A., and Banfield J. A. 1997. Biogeochemical weathering of silicate minerals. *Interactions between microbes and minerals*, , edited by Banfield J. F. and Nealson K. H. Reviews in Mineralogy, vol. 35. Washington, D.C.: Mineralogical Society of America. pp. 391–428.

Bennett P. C., Rogers J. R., Choi W. J., and Hiebert F. K. 2001. Silicates, silicate weathering, and microbial ecology. *Geomicrobiology Journal* 18:3–19.

Boison G., Mergel A., Jolkver H., and Bothe H. 2004. Bacterial life and dinitrogen fixation at a gypsum rock. *Applied and Environmental Microbiology* 70:7070–7077.

Boston P. J., Ivanov M. V., and McKay C. P. 1992. On the possibility of chemosynthetic ecosystems in subsurface habitats on Mars. *Icarus* 95:300–308.

Bunch T. E., Grieve R. A. F., Lee P., McKay C. P., Rice J. W., Jr., Schutt J. W., and Zent A. 1997. Haughton-Mars 97–II: Preliminary observations on highly shocked crystalline basement rocks from the Haughton impact crater. (abstract #1307). 29th Lunar and Planetary Science Conference. CD-ROM.

Chao E. C. T. 1968. Pressure and temperature histories of impact metamorphosed rocks, based on petrographic observations. *Neues Jahrbuch fuer Mineralogie. Abhandlungen* 108:209–246.

Cockell C. S. 2004. Impact-shocked rocks—Insights into archaean and extraterrestrial microbial habitats (and sites for prebiotic chemistry?). *Advances in Space Research* 33:1231–1235.

Cockell C. S. and Lee P. 2002. The biology of impact craters—A review. *Biological Reviews* 77:279–310.

Cockell C. S. and Osinski G. R. 2007. Impact-induced impoverishment and transformation of a sandstone habitat for lithophytic microorganisms. *Meteoritics & Planetary Science* 42:1985–1993.

Cockell C. S., Lee P., Osinski G. R., Horneck G., and Broady P. 2002. Impact-induced microbial endolithic habitats. *Meteoritics & Planetary Science* 37:1287–1298.

Cockell C. S., Lee P., Broady P., Lim D. S. S., Osinski G. R. R., Parnell J., Koeberl C., Pesonen L., and Salminen J. 2005. Effects of asteroid and comet impacts on habitats for lithophytic organisms—A synthesis. *Meteoritics & Planetary Science* 40:1901–1914.

de los Ríos A., Wierzchos J., Sancho L. G., and Ascaso C. 2002. Microhabitats and chemical microenvironments under saxicolous lichens growing on granite. *Microbial Ecology* 43:181–188.

Douglas S. and Beveridge T. J. 1998. Mineral formation by bacteria in natural microbial communities. *FEMS Microbiology Ecology* 26:79–88.

Ehrlich H. L. 1998. Geomicrobiology: Its significance for geology. *Earth-Science Reviews* 45:45–60.

Fike D. A., Cockell C. S., Pearce D., and Lee P. 2003. Heterotrophic microbial colonization of the interior of impact-shocked rocks from Haughton impact structure, Devon Island, Nunavut, Canadian High Arctic. *International Journal of Astrobiology* 1:311–323.

French B. M. 1998. *Traces of catastrophe*. Houston, Texas: Lunar and Planetary Institute. pp. 31–59.

Friedmann E. I. 1980. Endolithic microbial life in hot and cold deserts. Proceedings of the Fourth College Park Colloquium on Chemical Evolution: Origins of Life. Maryland.

Friedmann E. I. and Ocampo R. 1976. Endolithic blue-green algae in the Dry Valleys: Primary producers in the Antarctic desert ecosystem. *Science* 193:1274–1279.

Frisch T. and Thorsteinsson R. 1978. Haughton astrobleme: A mid-Cenozoic impact crater Devon Island, Canadian arctic archipelago. *Arctic* 31:108–124.

Grieve R. and Robertson P. B. 1979. The terrestrial cratering record I. Current status of observations. *Icarus* 38:212–229.

Gross M. G. 1971. Carbon determination. In *Procedures in sedimentary petrology*, edited by Carver R. C. New York: Wiley-Interscience. pp. 573–596.

Konhauser K. 1998. Diversity of bacterial iron mineralization. *Earth Science Reviews* 43:91–121.

Konhauser K. 2007. *Geomicrobiology*. Malden, MA: Blackwell Publishing.

Lindgren P., Parnell J., Bowden S. A., Taylor C., Osinski G. R., and Lee P. 2007. Preservation of organic carbon in impact melt breccias, Haughton impact structure. (abstract #1142). 38th Lunar and Planetary Science Conference. CD-ROM.

Mann H. B. and Whitney D. R. 1947. On a test of whether one of two random variables is stochastically larger than the other. *The Annals of Mathematical Statistics* 18: 50–60.

Martin W., Baross J., Kelley D., and Russel M. J. 2008. Hydrothermal vents and the origins of life. *Nature Reviews: Microbiology* 6:805–814.

McKnight P. E. and Najab J. 2010. Mann-Whitney U test. In *Corsini encyclopedia of psychology*, edited by Weiner I. B. and Craighead W. B. Hoboken, New Jersey: John Wiley & Sons. pp. 960–961.

Metzler A., Ostertag R., Redeker H.-J., and Stöffler D. 1988. Composition of the crystalline basement and shock metamorphism of crystalline and sedimentary target rocks at the Haughton impact crater, Devon Island, Canada. *Meteoritics* 23:197–207.

Naumov M. V. 1996. Impact-generated hydrothermal activity: The record in terrestrial craters. Proceedings, 27th Lunar and Planetary Science Conference. p. 935.

Oberson A. and Joner E. J. 2003. Microbial turnover of phosphorous in soil. In *Organic phosphorous in the environment*, edited by Turner B. L., Frossard E., and Baldwin D. S. Cambridge, Massachusetts: CABI Publishing, p. 147.

Omelon C. R. 2008. Endolithic microbial communities in polar desert habitats. *Geomicrobiology Journal* 25:404–414.

Osinski G. R. 2007. Impact metamorphism of $CaCO_3$-bearing sandstones at the Haughton structure, Canada. *Meteoritics & Planetary Science* 42:1945–1960.

Osinski G. R., Spray J. G., and Lee P. 2001. Impact-induced hydrothermal activity within the Haughton impact

structure, arctic Canada: Generation of a transient, warm, wet oasis. *Meteoritics & Planetary Science* 36:731–745.

Osinski G. R., Lee P., Spray J. G., Parnell J., Lim D. S. S., Bunch T. E., Cockell C. S., and Glass B. 2005a. Geological overview and cratering model for the Haughton impact structure, Devon Island, Canadian High Arctic. *Meteoritics & Planetary Science* 40:1759–1776.

Osinski G. R., Lee P., Parnell J., Spray J., and Baron M. 2005b. A case study of impact-induced hydrothermal activity: The Haughton impact structure, Devon Island, Canadian High Arctic. *Meteoritics & Planetary Science* 40: 1859–1877.

Osinski G. R., Cockell C. S., Lindgren P., and Parnell J. 2010. The effect of meteorite impacts on the elements essential for life. *AbSciCon 2010*:5252.

Osinski G. R., Tornabene L. L., Banerjee N. R., Cockell C. S., Flemming R., Izawa M. R. M., McCutcheon J., Parnell J., Preston L., Pickersgill A. E., Pontefract A., Sapers H. M., and Southam G. 2012. Impact-generated hydrothermal systems on Earth and Mars. *Icarus*, doi:10.1016/j.icarus.2012.08.030.

Parnell J., Osinski G. R., Lee P., Green P. F., and Baron M. J. 2005. Thermal alteration of organic matter in an impact crater and the duration of postimpact heating. *Geology* 33:373–376.

Parnell J., Boyce A., Thackrey S., Muirhead D., Lindgren P., Mason C., Taylor C., Still J., Bowden S., Osinski G. R., and Lee P. 2010. Sulfur isotope signatures for rapid colonization of an impact crater by thermophilic microbes. *Geology* 38:271–274.

Singleton A. C., Osinski G. R., McCausland P. J. A., and Moser D. 2011. Shock induced changes in density and porosity in shock metamorphosed crystalline rocks, Haughton-impact structure. *Meteoritics & Planetary Science* 46:1774–1786.

Stöffler D. 1966. Zones of impact metamorphism in the crystalline rocks of the Nördlinger Ries crater. *Contributions to Mineralogy and Petrology* 12:15–24.

Stöffler D. 1971. Progressive metamorphism and classification of shocked and brecciated crystalline rocks at impact craters. *Journal of Geophysical Research* 76:5541–5551.

Versh E., Kirsimäe K., and Jõeleht A. 2006. Development of potential ecological niches in impact-induced hydrothermal systems: The small-to-medium size impacts. *Planetary and Space Science* 54:1567–1574.

Vestal R. J. 1988. Biomass of the cryptoendolithic microbiota from the Antarctic desert. *Applied and Environmental Microbiology* 54:957–959.

Wackett L. P., Dodge A. G., and Ellis L. B. M. 2004. Microbial genomics and the periodic table. *Applied and Environmental Microbiology* 70:647–655.

Welch S. A., Barker W. W., and Banfield J. F. 1999. Microbial extracellular polysaccharides and plagioclase dissolution. *Geochimica et Cosmochimica Acta* 63:1405–1419.

Wierzchos J. and Ascaso C. 2001. Life, decay and fossilisation of endolithic microorganisms from the Ross Desert, Antarctica. *Polar Biology* 24:863–868.

SUPPORTING INFORMATION

Additional supporting information may be found in the online version of this article:

Table S1. Shock level categories based on petrographic analysis of crystalline (gneiss) rock. Adapted from Singleton et al. (2011).

Table S2. Sample coordinates shown in UTM as well as sample descriptions for all three suites of rocks utilized in this study.

Table S3. The total amount of organic carbon (% TOC) in Haughton target rocks and clast-rich melt rocks. Samples are from Suite 1 collection (see Methods section).

Table S4. Table shows XRF results depicting major oxide composition of sedimentary rocks from the Haughton crater.

Table S5. a) Table shows XRF and ICP results depicting major oxide composition of crystalline rocks from the Haughton Crater. b) Table shows ICP results depicting trace element composition of crystalline rocks from the Haughton Crater. Values beneath element symbols indicate detection limits. c) Calculated *Z*-values for select major oxide data for the crystalline samples using a nonparametric Mann–Whitney *U*-test. *Z*-values above 1.96 show significance at $P < 0.01$ (where P denotes probability), and values between 1.65 and 1.96 indicate significance at $P < 0.05$. An α of 0.05 was used, where α is the likelihood of error.